

A quantitative approach to deep-water sedimentation in the South China Sea : Changes since the last glaciation *

HUANG Wei (黄 维) and WANG Pinxian (汪品先)

(Laboratory of Marine Geology of State Education Commission , Tongji University , Shanghai 200092 , China)

Received August 18 , 1997

Abstract The first attempt is made to evaluate quantitatively the changes of accumulation rates in the South China Sea during the last glaciation and Holocene , based on the data of 72 sediment cores taken from six areas deeper than 100 m. As shown from the calculations , the accumulation rate during the last glaciation is much higher than that during the Holocene. The southern and northern continental slopes are distinguished from other areas by the highest accumulation rates , with different features of sedimentation for different stages : The Glacial-Holocene contrast in accumulation rate of terrigenous material is more distinct in the southern slope , while the contrast in biogenic sedimentation rate is more remarkable in the northern slope.

Keywords : South China Sea , accumulation rate , sedimentology , glacial cycle.

The marginal sea connects ocean and continent. Hence its sedimentation records the environment information both from the ocean and from the continent. Among the marginal seas of the West Pacific Ocean , it is in the South China Sea (SCS) where the AMS ^{14}C dating was first used to estimate the sedimentation rate^[1]. The change of sedimentation rates there in glacial cycles has attracted attention of many scientists^[2-4] , but the conclusions do not agree well with each other because the previous studies are mostly based on very few or even a single core site. For example , Broecker et al. ^[1] found a higher depositional rate during glacial and attributed it to dry climate then around the SCS , whereas Schönfeld and Kudrass^[4] believed that the glacial increase of terrigenous accumulation rates is insignificant and hence the hydrographic conditions at glaciation are similar to those of the modern. These conclusions become questionable today. A more complete data set is needed for better estimating the changes in sedimentation rates since the last glaciation and for drawing appropriate paleoenvironmental conclusion from it. Now , for the first time in the western Pacific , a quantitative analysis of deep-basin sedimentation becomes possible for the SCS , and the extensive research activities in the SCS since recent years by scientists from various countries have resulted in numerous sediment cores and vast amounts of chronological and lithological data of the cores , exceeding any other marginal sea in the region.

1 Materials and methods

A total of 72 sediment cores taken from the SCS over the years are used in the present study (fig. 1). Only the area deeper than 100 m is analyzed because the continent shelf was subjected to emergence and erosion at the glacial low sea-level stand. Our discussion is restricted to the deposition only during ^{18}O stages 1 and 2 for the limited length of piston and gravity cores.

* Project supported by the National Natural Science Foundation of China (Grant No. 49576268) .

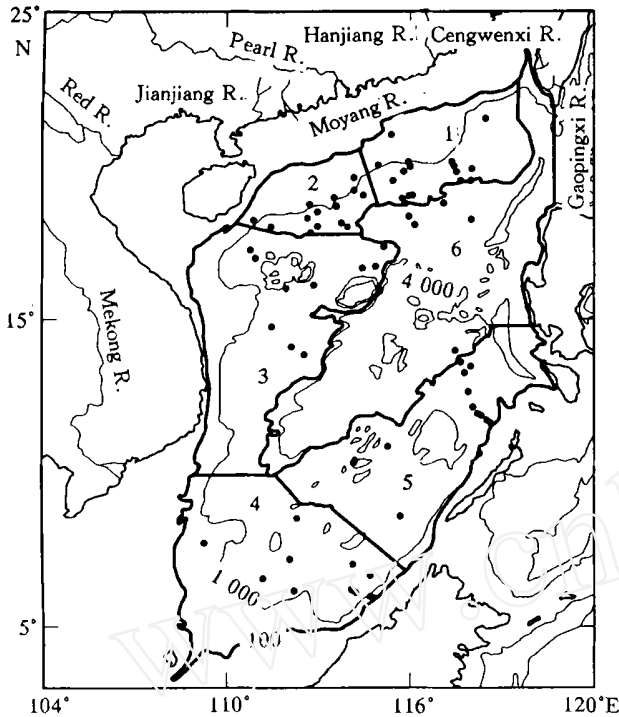


Fig. 1. Distribution of sediment cores and sediment areas in the deep-water part of the SCS. 1—6 denote six areas deeper than 100 m, black sites.

The chronology of the most sediment cores are based on oxygen isotope and carbonate stratigraphy using the time scale of Martinson et al. (e. g. ^{18}O stage 1: 0—12.05 ka B. P., ^{18}O stage 2: 12.05—24.10 ka B. P.)^[5], whereas the AMS ^{14}C datings are available only for some of cores. The sedimentation rate (thickness of sediment formed in unit time) and accumulation rate (volume of sediment accumulated on unit area in unit time) were calculated for different time intervals. The sediments in the SCS are mainly terrigenous and biogenic (carbonate and siliceous) in nature, and the accumulation rates were estimated for each of the components. Then the average accumulation rate and deposit volume can be calculated with 3-D interpolation on the assumption that the accumulation rates change smoothly between the core sites.

With its complicated bottom relief, the sediments in the SCS vary from area to area. According to the sediment types, carbonate contents^[6] and the variations in accumulation rate, six deposition areas (fig. 1) are distinguished in the deep-water part of the SCS, and the accumulation rates were calculated separately for each of the areas. They are the northeast slope area, east of the Pearl River mouth; the Northwest slope area, west of the Pearl River mouth and north of the Xisha Trough; the Vietnam offshore and Zhongsha area, east of Vietnam and west of the Central Basin of the SCS; the southern slope area, between the Nansha Islands and the Sunda shelf; the Nansha and the Sabah offshore area, including the Nansha Islands and area to the east; the Central Basin of the SCS, deeper than 3 500 m and below the carbonate lysocline.

2 Results

Due to the space limitation, the original data (including locations of the 72 core sites, water depths, references, datings and thickness of sediments for each stage) and results of calculations (sedimentation rates in cm/ka , total accumulation rates in $\text{g}/\text{cm}^2 \cdot \text{ka}^{-1}$, and accumulation rates of individual component for each stage) are omitted, but are available from the authors on request. The results are shown in table 1 and fig. 2. It should be noticed that there are only 13 sites provided with opal data, and there are no data from the Central Basin where the figures are extrapolated from its surrounding areas and hence may not represent the reality.

Table 1 The average deposit volume per year in the last glaciation (^{18}O stage 2 and Holocene (^{18}O stage 1) in deep-water areas of SCS (in 10^6t/a)

^{18}O stage	Total deposit volume	Deposit volume of terrigenous	Deposit volume of carbonates	Deposit volume of opal
1	92.0	79.4	21.9	4.6
2	167.4	155.6	22.4	13.3

3 Discussion

When the above results are compared with the discussions on sedimentation rates in the SCS in literature, some interesting conclusions about paleoenvironments during the last glaciation and Holocene can be drawn.

3.1 Total accumulation rate and supply of terrigenous clasts

As seen from table 1, the average annual deposit volume during the last glaciation distinctly exceeds that in the postglacial. The average total annual deposit volume is $167 \times 10^6 \text{ t/a}$ during ^{18}O stage 2 and $92 \times 10^6 \text{ t/a}$ during stage 1. As mentioned above, Schönfeld and Kudrass^[4] found that terrigenous accumulation rates during the last glaciation did not increase significantly compared with the modern ones. Their conclusion is based on oxygen isotope data of 13 piston cores from off the Pearl River mouth and off Sabah and is in contradiction to our findings. In fact, Schönfeld and Kudrass^[4] calculated the sedimentation rate for the long-time span of 110 800—18 300 a B. P. labeled as “last glaciation” (including ^{18}O stages 2, 3, 4 and 5a—d) and, thus were unable to find the glacial-postglacial contrast. The increase of the total sedimentation rate during the last glaciation is mainly ascribed to the non-carbonate component. The non-carbonate sedimentation rate during ^{18}O stage 2 is about double that in stage 1 while there is almost no change found in carbonate accumulation rate, despite of the significant increase of opal accumulation rate in stage 2 (table 1). However, the proportion of biogenic, especially opal, in the total deposit volume is very small.

During ^{18}O stage 1 (fig. 2(a)) the highest accumulation rate occurred in the northeast slope area with the average accumulation rate of $13.30 \text{ g/cm}^2 \cdot \text{ka}^{-1}$ followed by the southern slope with the rate of $6.42 \text{ g/cm}^2 \cdot \text{ka}^{-1}$. The accumulation rate was lower in other areas, being $2\text{—}5 \text{ g/cm}^2 \cdot \text{ka}^{-1}$ (fig. 2(a)). This pattern may be explained by the distribution of the rivers around the SCS. As shown in table 2, the highest silt discharge is provided by three of the rivers emptying into the SCS: the Mekong River, Red River and Pearl River. All other rivers of southern China, such as the Hanjiang River, Jianjiang River and Moyang River, are by far inferior to those three rivers in terms of silt discharge and drainage area. However, small rivers on uplifting islands may yield large amounts of sediments to the ocean^[7]: The Gaopingxi River and Cengwenxi River of the intensively rising Taiwan Island discharge as much silt to the sea as the Pearl River does, although their total drainage area measures only less than one percent of that of the Pearl River basin^[8,9] (table 2). Although the mud and silt carried by the Pearl River is transported westwards because of the Coriolis force, the accumulation rate in the northeast slope area is 3 times higher than in the northwest slope area (fig. 2(a), (b)), thanks to the mud and silt from Taiwan Island. Judging from the records of the shallow sedimentary trap (18°28' N, 116°01' E, 3 750 m) set up at 1 000 m depth, the sediment supply is subject to strong seasonal variations in the northern part

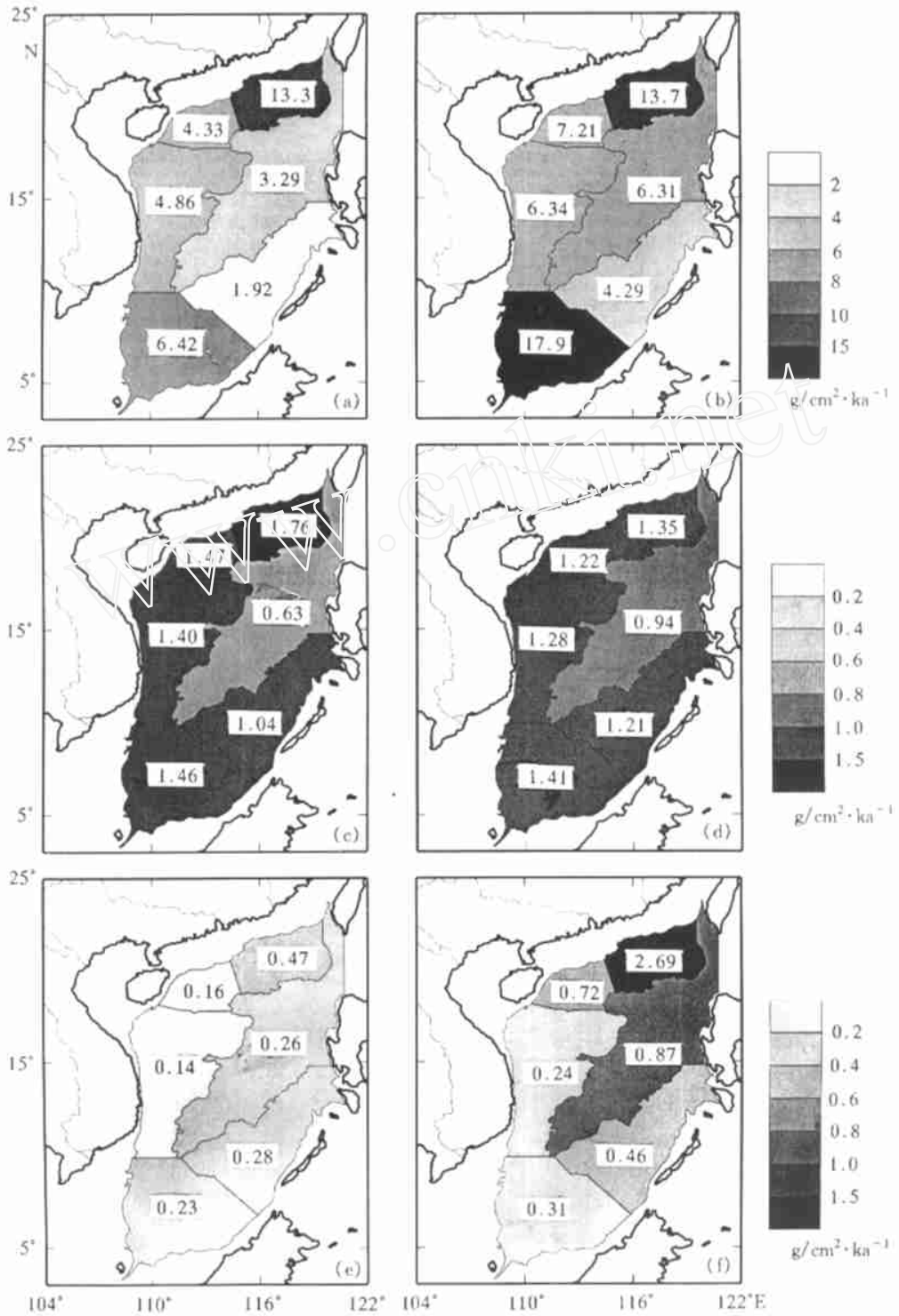


Fig. 2. Distribution of average accumulation rates in last glaciation (¹⁸O stage 2) and Holocene (¹⁸O stage 1) in the six deep-water areas of the SCS. (a), (b), Total accumulation rates in stages 1 and 2; (c), (d), carbonate accumulation rates in stages 1 and 2; (e), (f), opal accumulation rates in stages 1 and 2.

of the SCS. From November to February the vertical sedimentary flux reaches its maximum, which is well correlated to the winter wind speeds^[10,11], suggesting that a vast amount of terrigenous material was brought by currents driven by the strong winter wind, also increasing significantly the flux of biogenic sediment in the shallow sedimentary trap (see below). In stage 2, abundant terrigenous clasts could be brought by winter wind-induced currents through the Bashi Strait, the only connection between the SCS and Pacific Ocean then.

The accumulation rates of stage 2 are higher than those of stage 1 in all the six areas, maintaining the general pattern with highs in the northern and southern parts and a low in the central. Unlike stage 1, stage 2 accumulation rate in the southern slope area ($17.94 \text{ g/cm}^2 \cdot \text{ka}^{-1}$) is higher than that in the northeast slope area ($13.65 \text{ g/cm}^2 \cdot \text{ka}^{-1}$). Meanwhile, accumulation rates in all other areas are lower ($4-7 \text{ g/cm}^2 \cdot \text{ka}^{-1}$) (figure 2(b)).

The southern slope far exceeds other areas of the SCS by its glacial-Holocene contrast in the average accumulation rate, and this was caused mainly by the increased input of terrigenous but not biogenic sediment which did not change remarkably (fig. 2(c)–(f)). At the glacial sea-level low stand, there was a big river (the Sunda River) emptying into the SCS on the Sunda shelf, and the sediments carried by the Mekong River reached the deep-water area directly, deeply cutting into the exposed shelf sediments. All these must have brought a large quantity of terrigenous material to the area. By contrast, the accumulation rate remains nearly the same in the northeast slope area over the ^{18}O stages 1 and 2.

As shown by the calculations, the total annual deposit volume of terrigenous clast was $160 \times 10^6 \text{ t}$ in the deep-water area of the SCS during ice age (table 1), but the annual silt discharge to the SCS from only 8 modern rivers amounts to $500 \times 10^6 \text{ t}$ (table 2). At the glacial, the shelf was exposed and the rivers directly discharged to deep-water area, hence the deposit volume should be comparable to that of the river discharge. The low estimation of the glacial deposit volume here might be related to the turbidite activities. The sediment coring for paleoceanographic purposes is always kept away from the turbidite areas. Therefore, the calculations in the present study do not take turbidite deposition into account, and this might lead to underestimation of the deposit volumes.

Table 2 The runoff and silt discharge of some modern rivers emptying into the SCS

River	Drainage area (10^6 km^2)	River runoff/ $\text{km}^3 \text{ a}^{-1}$	Silt discharge/ 10^6 t a^{-1}	Reference
Mekong	0.719	470	160	[9]
Red	0.12	123	130	[9]
Pearl	0.45	349	83	[8]
Gaopingxi	0.003	9	39	[9]
Cengwenxi	0.001	2	28	[9]
Hanjiang	0.034	30	7	[9,12]
Jianjiang	0.009	8.5	1.9	[9,12]
Moyang	0.006	8.4	0.8	[9,12]

3.2 Accumulation rates of biogenic sediments

There are carbonate and siliceous biogenic sediments in the SCS. As shown in table 1, the average annual deposit volume of carbonate sediments in stage 2 ($22.4 \times 10^6 \text{ t/a}$) only slightly exceeds that in stage 1 ($21.9 \times 10^6 \text{ t/a}$). The carbonate sediments were subjected to severe

dissolution during the glacial cycle in the deep-water area of the SCS^[13] and, hence, can hardly provide information on the productivity changes. On the other hand, opal has not been subjected to any distinct dissolution cycle and can record the productivity variations more accurately. The sediment volume of opal has been changed quite significantly as shown in table 1: The volume of stage 2 (13.3×10^6 t/a) is nearly triple that of stage 1 (4.6×10^6 t/a), implying a considerable increase of productivity during the last glaciation.

Among the six deep-water areas of the SCS, the highest accumulation rates of biogenic sediment are found in the southern and northern slopes. During the ¹⁸O stage 1, the highest carbonate accumulation rate ($1.76 \text{ g/cm}^2 \cdot \text{ka}^{-1}$) was in the northeast slope area, declining to $0.6\text{--}1.5 \text{ g/cm}^2 \cdot \text{ka}^{-1}$ in other areas (fig. 2(c)). The siliceous accumulation rates are the highest in the northeast slope area ($0.47 \text{ g/cm}^2 \cdot \text{ka}^{-1}$) and much lower elsewhere (less than $0.3 \text{ g/cm}^2 \cdot \text{ka}^{-1}$) (fig. 2(e)). In stage 2, the maximal carbonate accumulation rates are found in the areas of southern slope and northeast slope ($1.41 \text{ g/cm}^2 \cdot \text{ka}^{-1}$ and $1.35 \text{ g/cm}^2 \cdot \text{ka}^{-1}$), varying from 0.9 to $1.3 \text{ g/cm}^2 \cdot \text{ka}^{-1}$ in other areas (fig. 2(d)). As to siliceous sediments, the highest values are in the area of northeast slope ($2.69 \text{ g/cm}^2 \cdot \text{ka}^{-1}$) in stage 2, much lower in any other areas ($0.2\text{--}0.9 \text{ g/cm}^2 \cdot \text{ka}^{-1}$) or in stage 1. When the biogenic accumulation rates are compared between the last glaciation and the Holocene, the most striking changes of opal accumulation rates occurred in the northern part of the SCS (including the northeast and northwest slopes), displaying a 4–6 times contrast (fig. 2(e), (f)). This might have been related to the influx of terrigenous material: The maximal biogenic sediment flux has been recorded by the shallow-water sediment trap in winter, corresponding to the high speeds of winter wind. This means that more terrigenous material can be carried by currents driven by the strong winter wind, and biogenic sediment flux increased thanks to the enhanced supply of nutrients^[10,11]. It is inferred, therefore, that the area with higher influx of terrigenous material has also a higher accumulation rate of biogenic sediment. The glacial enhanced winter monsoon was responsible for the significant glacial-postglacial changes in the opal accumulation rates in the northern part of the SCS.

4 Conclusions

1) The accumulation rate was higher during the last glaciation than during Holocene in deep-water parts (>100 m) of the SCS, and this is ascribed to the nearly doubling of the accumulation rate of terrigenous material there. The conclusion by Schönfeld and Kudrass^[4] about insignificant changes in accumulation rates during the last glaciation is not supported by calculations.

2) Among the six deep-water areas of the SCS, the glacial-Holocene contrast in the accumulation rate of terrigenous material is most distinct in the southern slope area, implying that the direct discharge of rivers into the slope during glacial was the main factor responsible for the increased accumulation rate. The recent palynological analysis in the southern part of the SCS indicates that the climate was not dry during glacial (personal communication by Sun Xiangjun and Li Xun, 1997), and it means that there is no reason to attribute the glacial increase of accumulation rate in the southern part of the SCS to dry climate as Broecker et al.^[1] did.

3) The carbonate accumulation rate has been little changed in the deep-water part of the SCS from glacial to Holocene, which is probably a result of compensation of enhanced surface productivity and increased deep-water carbonate dissolution. The opal accumulation rate during the last glaciation was 4–6 times higher than in the Holocene in the northern slope of the SCS, and this

might be explained by the increased productivity caused by the strengthened winter monsoon and enhanced supply of nutrients.

Acknowledgement Thanks are due to Dr. Jian Zhimin for providing the dry bulk density data and to Dr. Lin Huiling for opal analysis.

References

- 1 Broecker, W. S. , Andree, M. , Klas, M. et al. , New evidence from the South China Sea for an abrupt termination of the last glacial period , *Nature* , 1988 , 333 : 156 .
- 2 Wang Pinxian, Jian Zhimin, Liu Zhiwei , The sedimentation rates in South China Sea during late Quaternary , *Paleoceanary Research of South China Sea in Late Quaternary* (in Chinese) , Qingdao : Qingdao Ocean University Press , 1992 , 23 —41 .
- 3 Huang Wei , Wang Pinxian , Sedimentation in South China Sea since 150 000 a B. P. , *The South China Sea Since 150 000 a B. P.* (in Chinese) , Shanghai : Tongji University Press , 1995 , 33 —39 .
- 4 Schönfeld, J. , Kudrass, H. R. , Hemipelagic sediment accumulation rates in the South China Sea related to late Quaternary sea-level changes , *Quaternary Research* , 1993 , 40 : 368 .
- 5 Martinson, D. G. , Pisias, W. G. , Hays, J. D. et al. , Age dating and the orbital theory of the ice age : development of a high resolution 0 to 300 000 year chronostratigraphy , *Quaternary Research* , 1987 , 27 : 1 .
- 6 Su Guangqing , Wang Tianxing , Basic characteristics of modern sedimentation in South China Sea , *Oceanology of China Sea* , Dordrecht : Kluwer , 1994 , 2 : 407 .
- 7 Milliman, J. D. , Syvitski, J. P. M. , Geomorphic/ tectonic control of sediment discharge to the ocean : the importance of small mountainous rivers , *Jour. Geology* , 1992 , 100 : 525 .
- 8 Editorial Committee of Natural Geography of China , *Natural Geography of China —Surface Water* (in Chinese) , Beijing : Science Press , 1981 , 185 .
- 9 Milliman, J. D. , Meade, R. H. , World-wide delivery of river sediment to the ocean , *Jour. Geology* , 1983 , 91(1) : 1 .
- 10 Jennerjahn, T. C. , Liebezeit, G. , Kempe, S. et al. , Particle flux in the northern South China Sea , *Marine Geology and Geophysics of the South China Sea* , Beijing : China Ocean Press , 1992 , 228 —235 .
- 11 Chen Wenbin, Xu Luqiang, Jennerjahn, T. C. , Research on particle flux in northern South China Sea , *Sedimentation Progress and Geochemical in South China Sea* (in Chinese) , Beijing : China Ocean Press , 1993 , 191 —201 .
- 12 Feng Wenke , Xue Wangjun , Yan Dayuan , *Quaternary Geoenvironments in Northern South China Sea* (in Chinese) , Guangzhou : Guangdong Technology Press , 1988 , 261 .
- 13 Wang Pinxian , Wang Lijiang , Bian Yunhua et al. , Late Quaternary paleoceanography of the South China Sea : surface circulation and carbonate cycles , *Marine Geology* , 1995 , 127 : 145 .